Materials Science Research International, Vol.9, No.2 pp.167-173 (2003)

General paper

Effects of Cold Working and Heat Treatment on Transformation Temperature of Ti-41.7Ni-8.5Cu (at%) Shape Memory Alloy and Its Probabilistic Prediction

Maho HOSOGI*, Nagatoshi OKABE** Toshio SAKUMA***
and Shuichi MIYAZAKI****
* *Kagawa University, 2217-20, Hayashi-machi, Takamatsu, Kagawa 761-0396*
** *Ehime University, 3, Bunkyo-cho, Matsuyama, Ehime 790-8577*
*** *Central Research Institute of Electric Power Industry, 2-11-1, Iwado-kita, Komae, Tokyo 201-8511*
**** *University of Tsukuba, 1-1-1, Tennoudai, Tsukuba, Ibaraki 305-8573*

Abstract: The transformation temperatures of shape memory alloy vary with the composition and processing and manufacturing conditions of the alloy. The purpose of the present study is to clarify the effects of cold working and heat treatment on various transformation temperatures, and to estimate probabilistically the transformation temperatures by means of a model. The shape memory alloy used was Ti-41.7Ni-8.5Cu (at%), and the transformation temperatures were measured by the differential scanning calorimeter method (DSC method). The effects of processing and heat treatment on the transformation temperatures were investigated by changing the cold working ratio (10-40 %) and the heat treatment temperature (623-773 K), respectively. As a result, the transformation temperatures were found to decrease with increasing cold working ratio. The transformation temperatures were also found to increase with increasing heat treatment temperature. Therefore, the transformation temperatures were modeled by considering quantitatively the effects of the cold working ratio and the heat treatment temperature. A probabilistic prediction formula was proposed so that the reliability of the prediction may be estimated quantitatively.

Key words: *Shape memory alloy, Ti-Ni-Cu alloy, Transformation temperature, Cold working ratio, Shape memory treatment, Probabilistic prediction model*

1. INTRODUCTION

Ti-Ni-Cu alloys have been used in various fields because they have two unique functions: superelasticity and shape memory effect [1-3]. In the applications of shape memory alloys to actuators and heat engines, it is desired that the transformation temperature hysteresis is small in order to achieve rapid cyclic motion. As applicable alloys, the Ti-Ni-Cu system shape memory alloys are superior to other alloys such as the Ti-Ni system and the Cu system, and have been continuously developed as elements for energy conversion, because of their superior fatigue properties and corrosion resistance. From the viewpoint of thermal engine development, we have noted that the mechanical and functional properties of cyclic deformation behavior may be improved by adding copper to the Ti-Ni binary alloy, because the recovery stress increases with increasing Cu content, and both stress hysteresis and transformation strain decrease with increasing Cu content [4,5]. Furthermore, copper addition is effective for decreasing temperature hysteresis. The authors have already clarified that the most suitable com- position for realizing the required properties can be obtained at a Cu content of 8.5%. The development of a thermal engine requires transformation temperature data as fundamental design data for basic specifications.

The purpose of the present study is to clarify the effects of processing on the transformation temperature. First of all, the effects of cold working and shape memory heat treatment on the transformation temperature of Ti-41.7Ni-8.5Cu (at%) are investigated experimentally and formulated deterministically. Then, the probabilistic prediction formula is proposed so that the reliability of the prediction by our proposed formula may be estimated quantitatively.

2. MEASUREMENTS

The composition of the alloy used was Ti-41.7Ni-8.5Cu (at%). The wire alloy in DSC experiments was 1

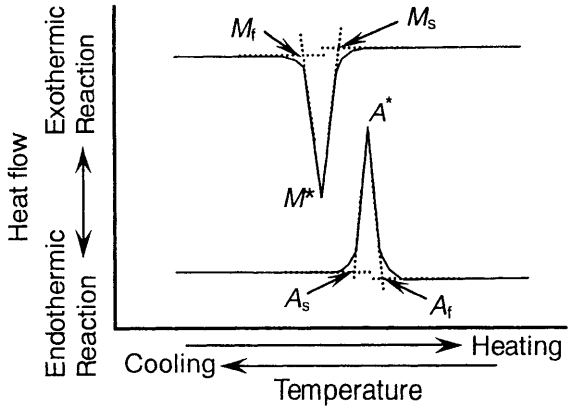

Fig.1. Schematic diagram of transformation temperature measurement by DSC method.

Received December 26, 2001
Accepted May 6, 2003

Original paper in Japanese was published in Journal of the Society of Materials Science, Japan, Vol. 51, No. 1 (2002) pp. 48-53.

mm in diameter, and was manufactured by repeatedly alternating cold extrusion and annealing of a hot forged bar from the ingot alloy. For the specimens subjected to heating at 673 K, cold working was performed at the cold working ratios, CW, of 10, 20, 30 and 40 %. For the specimens with CW of 30 %, heat treatment was performed at the temperatures of 623, 673, 723 and 773 K. Measurement of the transformation temperatures was conducted twice for each specimen by the DSC method, as shown schematically in Fig.1. Four transformation temperatures were defined, as shown in this figure.

3. RESULTS AND DISCUSSION

3.1. Effects of Cold Working and Shape Memory Heat Treatment on Transformation Temperature

Figure 2 shows the effect of CW on the transformation temperature. Four transformation temperatures A_f, A_s, M_s and M_f, were measured by DSC under stress-free conditions. The transformation temperatures decrease with increasing CW.

As CW increases, it becomes more difficult to induce martensite transformation, but easier to induce reverse transformation. This is because the internal strain energy due to cold working accompanying the increase of dislocations changes the critical driving force required for the phase transformation. Therefore, since the change of the transformation temperature may be considered to saturate together with the dislocation density due to cold working, the peak temperatures for both martensite transformation and reverse transformation, M^*_{CW} and A^*_{CW}, can be expressed by the following formula:

$$\begin{vmatrix} A^*_{CW} \\ M^*_{CW} \end{vmatrix} = \begin{vmatrix} A^*_{CW} - A^*_{\infty} \\ M^*_{CW} - M^*_{\infty} \end{vmatrix} \exp\left(-\frac{CW - 0.3}{CW_0} \right) + \begin{vmatrix} A^*_{CW\infty} \\ M^*_{CW\infty} \end{vmatrix}, \quad (1)$$

where A^*_{30} and M^*_{30} are the peak temperatures for the specimen with CW=30 %, A^*_{∞} and M^*_{∞} are the saturation temperatures of the lower limit for CW=∞, and CW_0 is a scale parameter for CW.

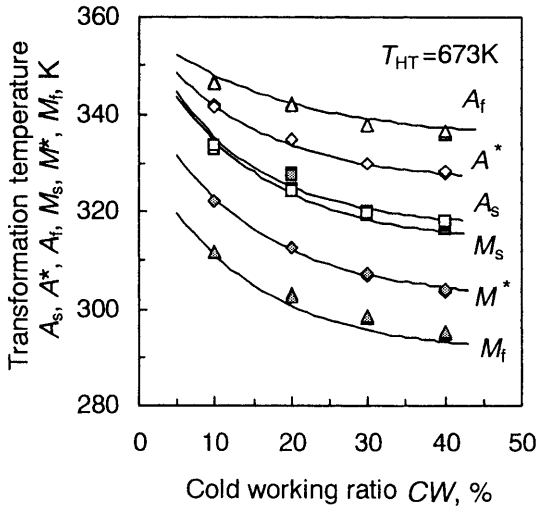

Fig.2. Effects of cold working ratio on the various transformation temperatures.

Figure 3 shows the influence of CW on the transformation temperature differences, ΔA_{CW} and ΔM_{CW}, between the start and end of transformation. ΔM_{CW} decreases slightly, while ΔA_{CW} increases with increasing CW and reaches saturation. It is considered that such a change of ΔA_{CW} might be caused by the impediment of the transformation progress due to the increase in dislocations during cold working. Therefore, from the above consideration, both ΔA_{CW} and ΔM_{CW} can be expressed as a function of CW by the following equation:

$$\begin{vmatrix} \Delta A_{CW} \\ \Delta M_{CW} \end{vmatrix} = \begin{vmatrix} A_f - A_s \\ M_s - M_f \end{vmatrix} = \begin{vmatrix} \Delta A_{CW30} - \Delta A_{CW\infty} \\ \Delta M_{CW30} - \Delta M_{CW\infty} \end{vmatrix} \exp\left(-\frac{CW - 0.3}{CW_0} \right) + \begin{vmatrix} A_{CW\infty} \\ M_{CW\infty} \end{vmatrix}, \quad (2)$$

where ΔA_{CW30} and ΔM_{CW30} are the temperature differences for the specimen with CW=30 %, which is the standard CW used in engineering working and therefore was selected as the standard CW value in the model, $\Delta A_{CW\infty}$ and $\Delta M_{CW\infty}$ are the saturation temperatures of the lower limit for CW=∞, and CW_0 is a scale parameter for CW. Using Eqs.(1) and (2), the effects of CW on transformation temperature can be expressed by the following equations:

$$\begin{vmatrix} A_{sCW} \\ A_{fCW} \end{vmatrix} = A^*_{CW} + \Delta A_{CW} \begin{vmatrix} m_{As} \\ m_{Af} \end{vmatrix}, \quad (3)$$

$$\begin{vmatrix} M_{sCW} \\ M_{fCW} \end{vmatrix} = M^*_{CW} + \Delta M_{CW} \begin{vmatrix} n_{As} \\ n_{Af} \end{vmatrix}, \quad (4)$$

where m_{As}, m_{Af}, n_{Ms} and n_{Mf} are defined below:

$$m_{As} = (A_s - A^*)/(A_f - A_s),$$
$$m_{Af} = (A_f - A^*)/(A_f - A_s),$$
$$n_{Ms} = (M_s - M^*)/(M_f - M_s),$$
$$n_{Mf} = (M_f - M^*)/(M_f - M_s).$$

We consider the scatter of various transformation temperatures quantitatively to discuss the reliability of the values predicted by Eqs.(3) and (4). Then their scatter can be estimated by using μ, which is the ratio of measured values to predicted values of the transformation temperatures for various CWs, as follows:

$$\mu = \frac{\text{Experimental data}}{\text{Predicted value}}.$$

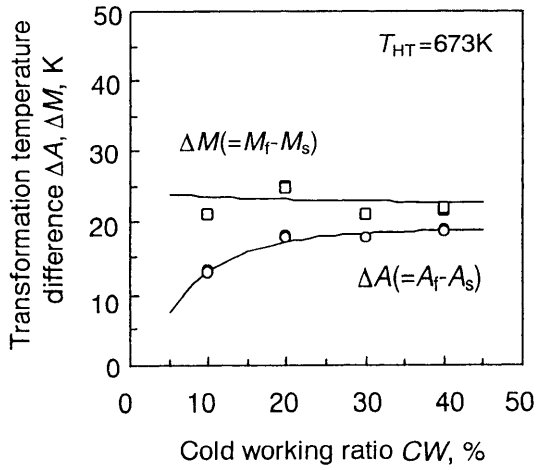

Fig.3. Effects of cold working ratio on the temperature differences.

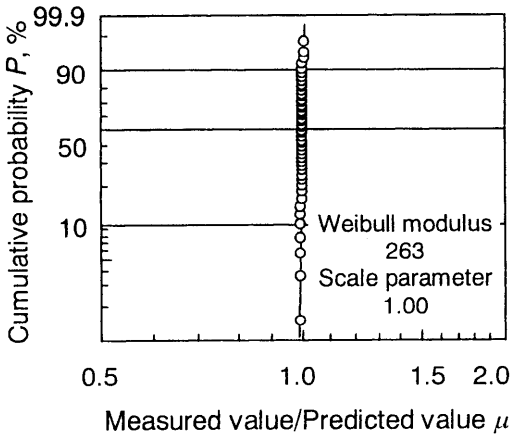

Fig.4. Weibull distribution of transformation temperature with various cold working ratios.

Figure 4 shows the Weibull plots of μ. The scatter can be well expressed by the 2-parameter Weibull distribution. The scale parameter is extremely small; namely, the scatter of the transformation temperature is found to be very small in Eqs.(3) and (4). Therefore, it is noted that the transformation temperatures can be well predicted deterministically by Eqs.(3) and (4) without considering their scatter.

Next, the effect of the heat treatment temperature on the transformation temperature is shown in Fig.5, where M^* and A^* represent the peak temperatures for both martensite transformation and reverse transformation, and T_{HT} represents the heat treatment temperature. It is found that both M^* and A^* increase linearly with the same slope with increasing T_{HT}. Temperature hysteresis gradually becomes narrow and saturates with increasing T_{HT}. These behavior seen in Fig.5 arise when strain energies in crystals are released through either rearrangement or disappearance of the dislocations generated during cold working by heat treatment, and hence the critical driving energy for both transformations change. Therefore, it can be understood that the effects of cold working on the transformation behavior are opposite to the effects of heat treatment temperature on the transformation behavior. Also in this case, using Eqs.(1) and (2), the effect of T_{HT} on $M^*_{T_{HT}}$ and $A^*_{T_{HT}}$ can be expressed by the following equation:

$$\begin{vmatrix} A^*_{T_{HT}} \\ M^*_{T_{HT}} \end{vmatrix} = a(T_{HT} - 673) + \begin{vmatrix} A^*_{T_{HT}673} \\ M^*_{T_{HT}673} \end{vmatrix}, \qquad (5)$$

where $M^*_{T_{HT}673}$ and $A^*_{T_{HT}673}$ are $M^*_{T_{HT}}$ and $A^*_{T_{HT}}$ for T_{HT}=673 K, which was experimentally estimated to fit the heat treatment temperature of the Ti-Ni-Cu alloy used in this experiment and is therefore treated as the standard temperature for modeling.

Figure 6 shows the effects of heat treatment temperature T_{HT} on the transformation temperature differences ($\Delta A_{T_{HT}}$, $\Delta M_{T_{HT}}$) between the start and end of transformation. Both $\Delta A_{T_{HT}}$ and $\Delta M_{T_{HT}}$ tend to decrease exponentially and rapidly with increasing heat treatment temperature. Such tendencies of transformation temperatures can be inferred by considering that the increase of heat treatment temperature may promote the growth of such new formation phases as the martensite phase and the parent phase because cold working strain energy is released during heat treatment.

Therefore, it can be understood that the effects of cold working are opposite to the effects of heat treatment temperature on the transformation behavior. The release of cold working strain energies by heat treatment saturates with increasing heat treatment temperature, and the effect of heat treatment temperature on the changes of $\Delta A_{T_{HT}}$ and $\Delta M_{T_{HT}}$ saturates at the same time. Therefore, the behavior of $\Delta A_{T_{HT}}$ (=A_f-A_s) and $\Delta M_{T_{HT}}$ (=M_s-M_f) with

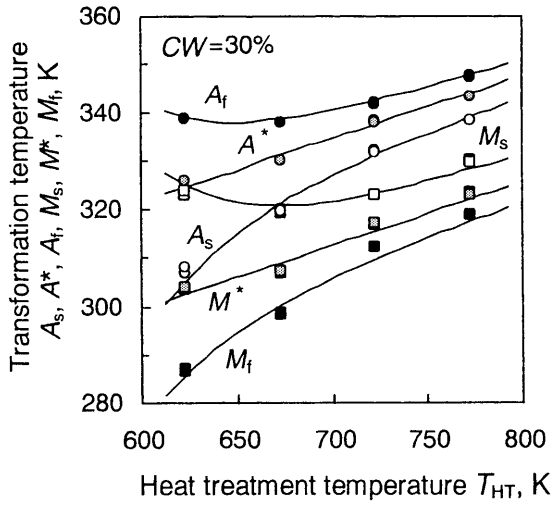

Fig.5. Effects of the heat treatment temperature on the various transformation temperatures.

increasing T_{HT} is given by the following equation:

$$\begin{vmatrix}\Delta A_{T_{HT}}\\ \Delta M_{T_{HT}}\end{vmatrix} = \begin{vmatrix}A_f - A_s\\ A_s - A_f\end{vmatrix} = \begin{vmatrix}\Delta A_{T_{HT}673} - \Delta A_{T_{HT}\infty}\\ \Delta M_{T_{HT}673} - \Delta M_{T_{HT}\infty}\end{vmatrix}\exp\left(-\frac{T_{HT}-673}{T_{HT0}}\right) + \begin{vmatrix}\Delta A^*_{T_{HT}\infty}\\ \Delta M^*_{T_{HT}\infty}\end{vmatrix} \quad (6)$$

In addition, using Eqs.(5) and (6), the effect of T_{HT} on transformation temperatures can be expressed by the following equations:

$$\begin{vmatrix}M_{sT_{HT}}\\ M_{fT_{HT}}\end{vmatrix} = M^*_{T_{HT}} + \Delta M_{T_{HT}}\begin{vmatrix}n_{Ms}\\ n_{Mf}\end{vmatrix}\exp\left(-\frac{T_{HT}-673}{T_{HT0}}\right) \quad (7)$$

$$\begin{vmatrix}A_{sT_{HT}}\\ A_{fT_{HT}}\end{vmatrix} = A^*_{T_{HT}} + \Delta A_{T_{HT}}\begin{vmatrix}m_{As}\\ m_{Af}\end{vmatrix}\exp\left(-\frac{T_{HT}-673}{T_{HT0}}\right) \quad (8)$$

Now, let us consider the scatter of transformation temperature quantitatively to discuss the reliability of the values predicted by Eqs.(7) and (8). Their scatter can be estimated by using μ, which is the ratio of measured values to predicted values of the transformation temperatures for various T_{HT}. Figure 7 shows the Weibull plots of μ for various T_{HT}. The scatter of the transformation temperature is extremely small. Therefore, the transformation temperature can also be predicted deterministically by Eqs.(7) and (8).

3.2. Effects of Cold Working and Heat Treatment Temperature on Transformation Heat Energy

Figure 8 shows the effect of CW on the reverse transformation heat energy, E_A, and the transformation heat energy, E_M. Figure 9 shows the effect of the heat treatment temperature T_{HT} on E_A and E_M. E_A and E_M decrease with increasing CW, and increase with increasing T_{HT}. We assume that E_A is equal to E_M for various CWs and T_{HT}s, and the behavior of E_A with CW can be expressed by the following equation:

$$E_{CW} = (E_{CW30} - E_{CW\infty})\exp\left(-\frac{CW-0.3}{CW_0}\right) + E_{CW\infty} \quad (9)$$

$$E_{T_{TH}} = (E_{T_{TH}673} - E_{T_{TH}\infty})\exp\left(-\frac{T_{HT}-673}{T_{HT0}}\right) + E_{TH\infty} \quad (10)$$

where E_{CW30} and $E_{CW\infty}$ are respectively the transformation heat for CW=30 % and the saturation transformation heat for CW=∞, $E_{T_{HT}673}$ and $E_{T_{HT}\infty}$ are the transformation heat for T_{HT}=673 and the saturation transformation heat for T_{HT}=∞, and T_{HT0} is a scale parameter.

Figure 10 shows the Weibull distribution of μ ratio

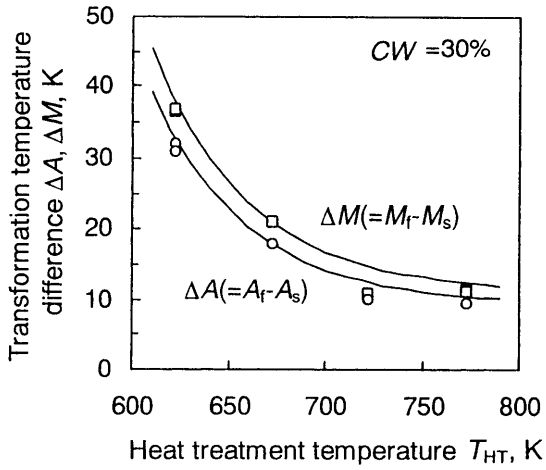

Fig.6. Effects of the heat treatment temperature on the transformation temperature differences.

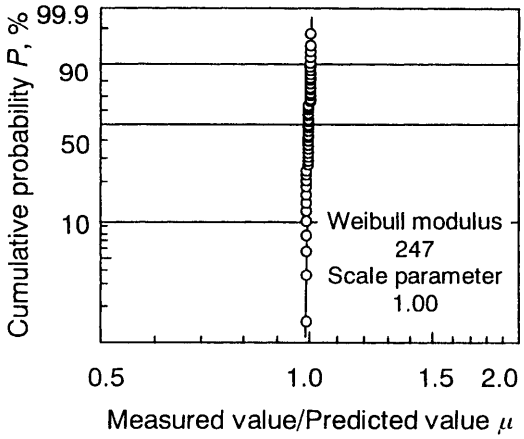

Fig.7. Weibull plots of μ that is defined by the measured value/predicted ones of transformation temperature for T_{HT}.

of E_A and E_M for various CWs and T_{HT}s. Namely, μ is the ratio of measured data to predicted ones. It is obvious from Fig.10 that CW exerts greater effects than T_{HT} on the scatter of transformation heat. These effects will be discussed in the probabilistic prediction of the variation of transformation heat in section 4.

3.3. Transformation Temperature Properties and Their Use in the Prediction of Transformation Heat Energy

Figure 11 shows the effects of A_s and M_f on various transformation temperature differences, ΔA and ΔM. This figure indicates that A_s is related to the heat energy that is given off at the start of the reverse transformation, and that M_f is related to the heat energy remaining in the alloy at the end of martensite transformation. It can be inferred that ΔA is related to the thermal energy from the environment while reverse transformation occurs, and ΔM is related to the thermal energy discharged to the

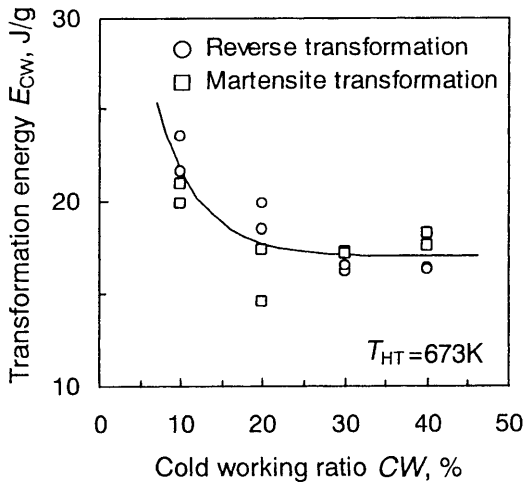

Fig.8. Effect of the cold working ratio on the transformation heat of E_A and E_M.

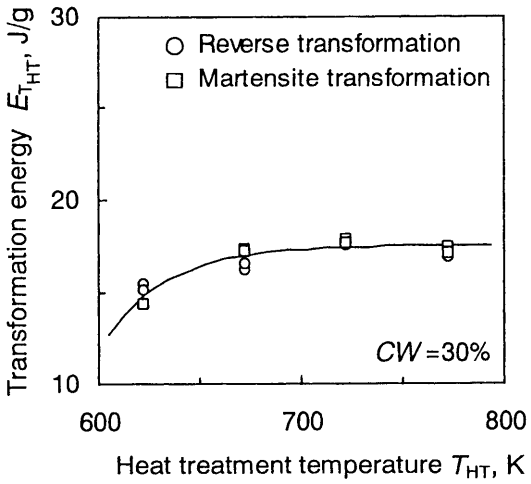

Fig.9. Effect of the heat treatment temperature on the transformation heat of E_A and E_M.

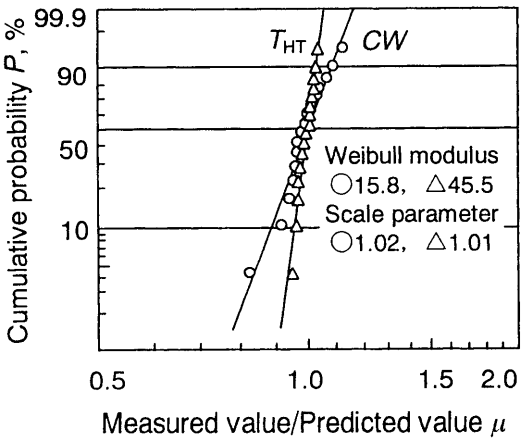

Fig.10. Weibull distributions of μ ratio of E_A and E_M in various CW and T_{HT} as ratio of measured value to predicted one.

environment. In Fig.11, it is seen that ΔA and ΔM decrease with increasing A_s and M_f. In other words, the overheating temperature range in which energy is absorbed from the environment decreases as the potential energy at the start of reverse transformation increases, and the overcooling temperature range in which energy is discharged to the environment decreases as the potential energy at the end of the martensite transformation increases. The relationship between ΔA and A_s can be expressed by the following formula, as can the relationship between ΔM and M_f.

$$\left|\frac{\Delta A}{\Delta M}\right| = \left|\frac{A_f - A_s}{A_s - A_f}\right| = a\left|\frac{A_t - 300}{M_t - 300}\right| + \left|\frac{\Delta A_{300}}{\Delta M_{300}}\right| . \quad (11)$$

Figure 12 shows the Weibull distribution of the transformation temperature differences, $\mu_{\Delta A}$ and $\mu_{\Delta M}$, which are the ratios of measured values to predicted values. The error in the prediction of ΔA and ΔM on the basis of A_s and M_s is large, as shown in Fig.12, but is well fitted by the Weibull distribution. Then, both ΔA and ΔM can be probabilistically predicted, considering the confidence interval, as described in section 4. On the other hand, considering the relationships of E_A and E_M with the ratio R_t of ΔA to A_s and ΔM to M_f, E_A and E_M decrease along their respective straight lines with decreasing R_t, as shown in Fig.13. The relationship between transformation heat energies and R_t at various CWs and T_{HT}s is expressed as:

$$E_{CW} = a(R_t - 0.05) + E_{CW0.05} , \quad (12)$$

$$E_{T_{TH}} = b(R_t - 0.05) + E_{T_{HT}0.05} . \quad (13)$$

The values predicted by Eqs.(12) and (13) are well fitted by the Weibull distribution, as shown in Fig.14, and show

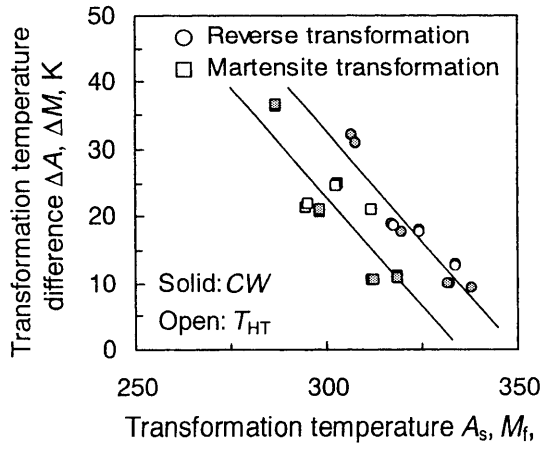

Fig.11. Effects of A_s and M_f on transformation temperature differences.

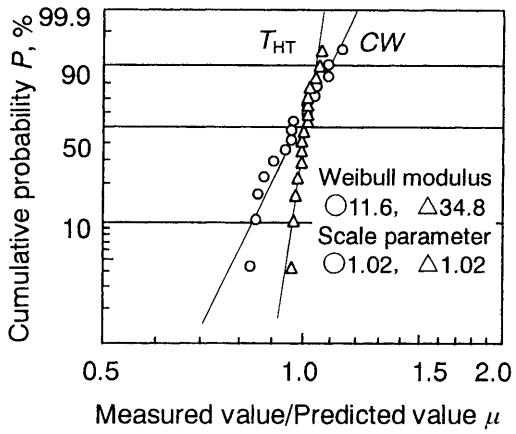

Fig.12. Weibull distributions of μ normalized ΔA and ΔM as ratio of measured value to predicted one.

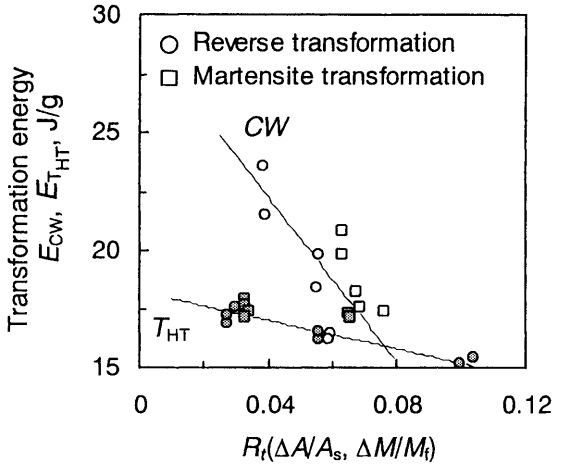

Fig.13. Effects of both ratios R_t of ΔA to A_s and ΔM to M_f on each transformation heat.

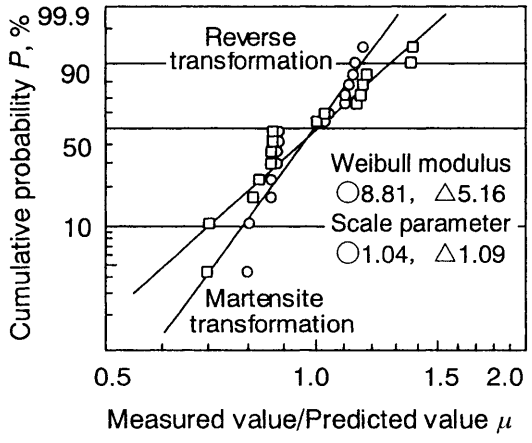

Fig.14. Weibull distributions of μ ratio of E_A and E_M as ratio of measured value to predicted one.

small scatter. Therefore, good predictions can be achieved by using these equations.

4. FUNDAMENTAL CONCEPTS OF VALUE SCATTER AND APPLICATION TO RELIABILITY DESIGN

Every Weibull distribution described above can be analyzed using the ratio μ of the experimental data to the predicted value as a scatter parameter. Therefore, using X for the values of various properties such as A_s, A_f, M_s, M_f, ΔM and ΔA, X can be estimated probabilistically according to probability P, by the following equation:

$$X(P) = X_0 F^{-1}(P), \tag{14}$$

where X_0 is a deterministic value predicted by various equations as a function of T_{HT} or CW, and $F^{-1}(P)$ is equivalent to the probability variable $\mu(=X/X_0)$ with a shape parameter m and a scale parameter μ_0 and is given by the following equation:

$$F^{-1}(P) = \mu = \mu_0 \sqrt[m]{\ln(1-P)^{-1}}. \tag{15}$$

In contrast, in the first functional design of a heat engine using shape memory alloy, the optimization of heat hysteresis, ΔM and ΔA, is required depending on the heat source available for it. CW and T_{HT} are used to adjust the optimization, because they have a large influence on ΔM and ΔA. Therefore, when all values of X_0 for transformation temperatures A_f, A_s, M_s and M_f, and transformation temperatures differences, ΔM and ΔA, are predicted on the basis of CW and T_{HT} according to a functional design specifications, at the confidence interval P_c (example:90 %), the predicted value X is in the range given by

$$X_0 F^{-1}(0.05) < X < X_0 F^{-1}(0.95). \tag{16}$$

Also for heat hysteresis, ΔM and ΔA, as well as transformation heat energies, E_A and E_M, of the shape memory alloys at arbitrary T_{HT}, CW should be predicted probabilistically from the viewpoint of reliability design, according to reliability, R (example:99.99 %). The predicted value, X, exists in the range given by

$$X = X_0 F^{-1}(1-P) = X_0 F^{-1}(0.0001). \tag{17}$$

The probabilistic estimation method proposed herein is very useful for reliability design of a heat engine that requires probabilistic estimation from the point of view of functional reliability.

5. CONCLUSIONS

The effects of processing and heat treatment conditions on the transformation temperatures were investigated. The behavior of various transformation tem-

peratures and transformation heat energies were modeled, considering the effects of cold working and heat treatment, to predict probabilistically the scatter of measured values and the confidence interval of the values assumed from the proposed model.

In the design of a reciprocating heat engine that uses shape memory alloy Ti-Ni-Cu as an energy conversion element, the fundamental properties of transformation temperature under the stress-free condition must be known and used as initial design data to determine the basic specifications of the heat engine. In this case, the effects of cold working and heat treatment on the fundamental properties of transformation temperatures measured by the DSC method must be estimated quantitatively, including their scatter. Therefore the relationships for the transformation temperatures and the transformation heat energies with cold working and heat treatment were modeled as Eqs.(3), (4), (7) and (8). The results obtained are summarized as follows:

(1) The transformation temperatures, A_f, A_s, M_s and M_f, decrease with increasing CW. The relationships between transformation temperatures and CW can be formulated as Eqs.(3) and (4).

(2) Both reverse transformation temperatures and martensite transformation temperatures show the same decreasing tendency with increasing CW that can be represented by Eqs.(3) and (4).

(3) The cold working ratio has the opposite tendency to the shape memory heat treatment concerning the effect on transformation heat energy. The behavior of transformation heat energy with increasing CW and shape memory heat treatment temperature can be represented by Eqs.(9) and (10).

(4) The martensite transformation temperature range ΔM and reverse transformation temperature range ΔA tend to decrease with increasing M_f and A_s.

(5) The scatter of the ratio μ of measured data X to values X_0 predicted using modeling equations (3), (4), (7), (8), (9) and (10) can be well fitted by the Weibull distribution. Modeling equation (14) was derived to probabilistically predict various transformation temperatures and energies required for a heat engine.

(6) Modeling equation (14), which can be used to analyze the confidence level and the reliability from the predicted transformation temperature and temperature hysteresis, can be applied to functional reliability design of a heat engine using shape memory alloy.

REFERENCES

1. T. Honma, Jour. Jpn. Soc. Mech. Eng., **87**-786, (1984) 517.
2. K. Yamaguchi, Jpn. Inst. Met., **32**-7, (1993) 495.
3. M. Miyagi, Jpn. Inst. Met., **24**-1, (1985) 69.
4. S. Miyazaki, K. Mizukoshi, T. Ueki, T. Sakuma and Y. Liu, Mater. Sci. and Eng., **A273**-275, (1999) 658.
5. T. Sakuma, U. Iwata, H. Takaku, N. Kariya, Y. Ochi and T. Matsumura, Trans. Japan Soc. Mech. Eng. **A66**-644, (2000) 748.